www.czasopisma.pan.pl PAN www.journals.pan.pl
Chemical and Process Engineering 2019, 40 (1), 39–47
DOI: 10.24425/cpe.2018.124995

Numerical modelling of ozonation process with respect to bromate formation. Part II – Model validation

Urszula Olsińska*

AQUA SEEN Spółka z o.o., ul. Siennicka 29, 04-394 Warszawa, Poland

Validation results of a theoretical model that describes the formation of bromate during ozonation of bromide-containing natural waters are presented. An axial dispersion model integrating the non-ideal mixing, mass-transfer and a kinetic model that links ozone decomposition reactions from the Tomiyasu, Fukutomi and Gordon ozone decay model with direct and indirect bromide oxidation reactions, oxidation of natural organic matter and reactions of dissolved organics and aqueous bromine was verified. The model was successfully validated with results obtained both at a laboratory and a full scale. Its applicability to different water supply systems was approved.

Keywords: model, ozonation, bromate, hydrodynamics, kinetics, validation

1. INTRODUCTION

In the last two decades, a great interest has been focused on the development of models to estimate the formation and fate of disinfection by-products in water foreseen for human consumption. To date, several models for predicting DBPs have been reported in the scientific literature and reviewed by Chowdhury et al. (2009) and Sadiq and Rodriguez (2004). In addition, models dedicated to bromate formation were carefully assessed by Jarvis et al. (2007) in terms of their applicability to real water. The authors pointed out the main advantages and disadvantages of the reviewed models. They found that none of the models can be considered accurate for generically predicting bromate formation at water treatment plants.

Recently, a numerical mechanistic model (ADM), which may potentially be used for prediction of bromate formation at an individual WTW, has been developed (Olsińska, 2019). In the proposed model reactions of ozone self-decomposition (TFG mechanisms), direct and indirect reactions of bromide oxidation, and competitive reactions of dissolved ozone and radicals with various constituents present in natural waters (e.g. carbonate species, natural organic matter, phosphates, ammonia) have been included. Apart from the kinetic model such phenomena as convection in liquid and gas phases, ozone mass transfer from gas to liquid phase and mixing in both fluids have been considered. In order for the model to be considered for application at WTW, it must be validated with real data.

Thus, the main purpose of the study presented herein was to verify the theoretical model developed elsewhere (Olsińska, 2019) with data collected in experiments carried out both in a laboratory and at water treatment plants, where ozone contactors are operated under different hydraulic conditions, and ozonated water contained bromide ions.

* Corresponding author, e-mail: urszula.olsinska@gmail.com

2. EXPERIMENTAL METHODS

2.1. Experimental set-up

Several experiments were performed in a laboratory and full-scale for the sake of model validation. The installation employed under laboratory conditions consisted of a continuous-flow bubble contactor with a total column height of 1.8 m and a nominal diameter of 0.05 m, feed water tank, gas preparation system, and pH correction system. The ozone contactor was operated at the co- and counter-current flow mode. The feed gas was prepared from the air by means of PSA oxygen generator (As-12, AirSep Corporation) connected in-series with the ozone generator (EFFIZON® SWO 30/15, OZOMATIC GmBH) and then dispersed in water next to the bottom of the column. The fine-bubble membrane diffuser with pores of 0.45μm in diameter was used as the gas sparger. The diffuser was elevated 7 mm from the bottom of the column. Since the tests were assumed to be conducted under conditions of established steady-state flow, the water depth was maintained constant at 1.6 m using an overflow weir (a system of V-notch weirs) placed at the top of the column. To control/measure water and gas flow rates rotameters were installed. The pH correction system comprised a dosing pump followed by a static mixer installed at the outlet from the feed water tank. The pH of water was adjusted using dilute sodium hydroxide or sulphuric acid solutions.

The applicability of the model was tested against the experimental data obtained from field-scaled investigations as well. These tests were performed at four surface water treatment plants (one with two separate treatment trains), where pre-ozonation and/or post-ozonation steps are incorporated into their treatment lines. The ozonation units differ in geometry and gas dispersion modes. Ozone is dispersed in the liquid phase using either fine bubble diffusers, an emulsifier or turbines (Fig. 1).

2.2. Tracer tests

To evaluate the hydrodynamic behaviour of the reactor tracer tests (Levenspiel, 1999) were performed for the liquid phase. Particularly, they were done to determine experimentally the longitudinal (axial) dispersion coefficients, which uniquely characterises the degree of backmixing during the flow. A pulse of a concentrated solution of a non-reactive red dye Rhodamine A (the lab-scale experiments) or sodium chloride (full-scale experiments) was rapidly injected upstream of the water inlet point into the contactor. The concentration of the tracer in samples collected from the effluent exit line was measured using the colorimetric or conductometric method. Closed vessel boundary conditions were maintained in all experiments on residence time distribution. Based on the exit age distribution (the E curve) a mean residence time, variance of dimensionless time and finally a vessel dispersion number were computed (Levenspiel, 1999; Olsińska, 2002).

2.3. Analytical methods

All anions of consideration were determined by a high-performance ion chromatography. Measurements were carried out by means of Dionex DX 500 (Dionex Co., USA) ion chromatograph, equipped with IonPac AG 23 (2 × 50 mm) guard column connected in series with analytical column IonPac AS23 (2 × 250 mm). Bromates were evaluated in line with the ISO 11206 standard (2011). The DOC content was measured using TOC/AOX 1200 Analyzer version 4.2.1 (Thermo Electron Co., The Netherlands) in water samples passing 0.45 mm filters prior to analysis. The water pH was monitored using 692 pH/ion meter (Metrohm, Germany). The tests were performed at ambient temperature, which was measured continuously throughout the experiments. The experiments were replicated at least three times and each chemical analysis was performed at least in triplicate. The samples' means were calculated.

A – WTP at Strumień (pre-ozonation step)

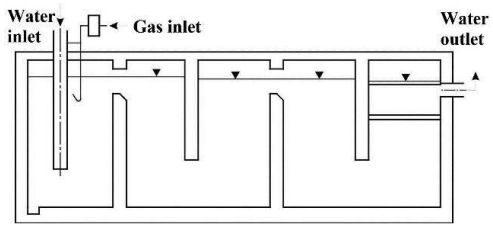

B – WTP at Strumień (post-ozonation step)

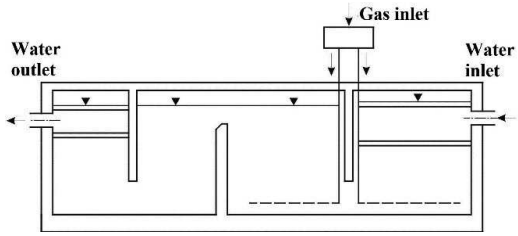

C – WTP at Dziećkowice (pre-ozonation step)

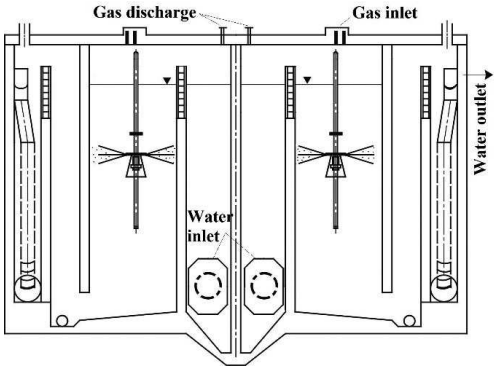

D – WTP at Dziećkowice (post-ozonation step)

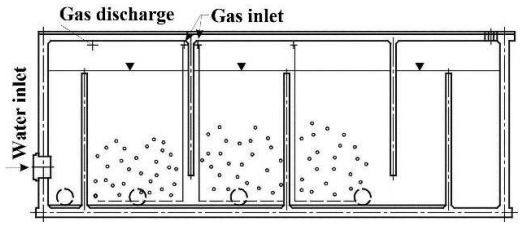

E – WTP at Goczałkowice (pre-ozonation; 1st)

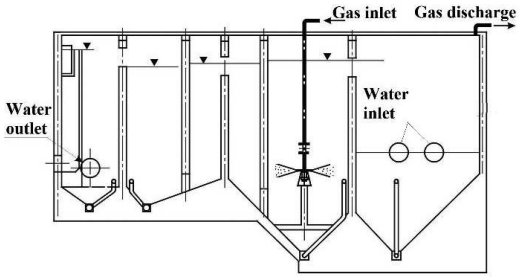

F – WTP at Goczałkowice (pre-ozonation, 2nd)

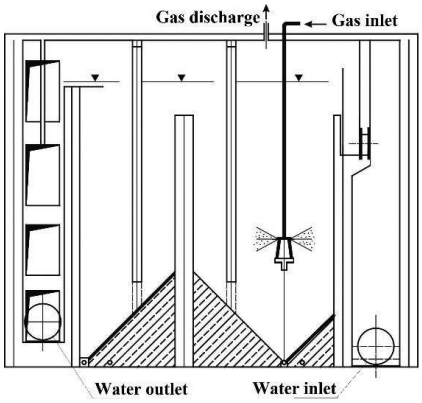

Fig. 1. Schematic of ozone contactors used at Dziećkowice, Strumień and Goczałkowice

3. RESULTS AND DISCUSSION

3.1. Model input parameters

The model includes several independent state variables. Thus, the definition of a few input values of these variables was required before integration started. First, a gas hold-up coefficient was determined. In the two-phase vertical uniform bubble flow system, a concept of slip velocity as proposed by Lapidus and Eglin (1957) was adopted:

$$u_s = \frac{u_G}{\varepsilon_G} \pm \frac{u_L}{\varepsilon_L} = u_p f(\varepsilon_G) \tag{1}$$

where $f(\varepsilon_G)$ is a function of the gas hold-up coefficient (Davidson and Harrison, 1966; Griffith and Wallis, 1961) and u_p is a terminal bubble rise velocity. However, for superficial gas velocities lower than 5 cm·s^{-1}, the effect of the gas hold-up can usually be neglected (Biń et al., 2001; Turner, 1966). The bubble rise velocity depends on physical properties of the liquid and bubble size. The latter was estimated using

empirical formulas proposed by Akita and Yoshida (1974), and Mariñas et al. (1993). Then the bubble rise velocity was approximated by a correlation derived by Clift et al. (1978), while outside the range of its applicability an expression suggested by Mendelson was introduced in the model (Roustan et al., 1993). Finally, the mean value of the gas hold-up coefficient was computed and as such it was used in a numerical solution of the model tested.

Additionally, in case of the co-current flow downward the vertical pipe (case A) the bubble size was calculated using a correlation established by Hinze (1955) with u_p pre-determined according Harmathy's formula (1960). Where turbines were used as gas spargers, an expression derived by Calderbank (1967) was applied to estimate the bubble Sauter diameter. The estimated bubble diameters were also used to determine a specific gas-liquid interfacial area, which was computed assuming a spherical shape of the gas bubbles ($a = 6\varepsilon_G/d_b$).

The defined values of the input variables are reported in Table 1 and Table 2, respectively, for the laboratory tests and those performed at the facilities operated at the full-scale. The pressure at the top of the contactors investigated in this study was assumed to be 101325 Pa.

Table 1. Input parameters – laboratory-scale experiments

Parameter	Co-current flow mode			Counter-current
	I (pH = 6.98)	II (pH = 7.85)	III (pH = 8.93)	IV (pH = 7.84)
$[O_3]_{G,0}$, mol·m^{-3}	5.625×10^{-2}	7.583×10^{-2}	6.542×10^{-2}	7.583×10^{-2}
$[DOC]_0$, mol·m^{-3}	2.091×10^{-1}	2.733×10^{-1}	2.508×10^{-1}	2.733×10^{-1}
$[H^+]_0$, mol·m^{-3}	1.047×10^{-4}	1.413×10^{-5}	1.175×10^{-6}	1.445×10^{-5}
$[OH^-]_0$, mol·m^{-3}	9.550×10^{-5}	7.079×10^{-4}	8.511×10^{-3}	6.918×10^{-4}
$[Br^-]_0$, mol·m^{-3}	1.252×10^{-3}	1.252×10^{-3}	1.252×10^{-3}	1.252×10^{-3}
$[PO_4^{3-}]_0$, mol·m^{-3}	1.519×10^{-2}	1.602×10^{-2}	1.496×10^{-2}	1.603×10^{-2}
$[HCO_3^-]_0$, mol·m^{-3}	1.589	1.557	1.393	1.554
$[CO_3^{2-}]_0$, mol·m^{-3}	0	0	0.194	0
$[NH_4^+]_0$, mol·m^{-3}	1.83×10^{-2}	1.94×10^{-2}	1.87×10^{-2}	1.94×10^{-2}
$[NH_3]_0$, mol·m^{-3}	– | $8.81 \times 10^{-3*}$	– | $8.81 \times 10^{-3*}$	– | $8.81 \times 10^{-3*}$	–
T, K	289.0	286.4	288.3	286.8
D_{O_3}, m^2 s^{-1}	1.62×10^{-9}	1.60×10^{-9}	1.61×10^{-9}	1.60×10^{-9}
d_b, m	0.0035	0.0035	0.0035	0.0035
k_La, s^{-1}	3.08×10^{-2}	3.08×10^{-2}	3.08×10^{-2}	2.93×10^{-2}
H_e, Pa·m^3·mol^{-1}	8.15×10^6	7.13×10^6	7.86×10^6	7.32×10^6
ε_G, –	0.081			0.090
ε_L, –	0.919			0.910
D_{LL}, m^2·s^{-1}	1.19×10^{-3}			1.46×10^{-3}
u_L, m·s^{-1}	0.0042			0.0032
u_{G_0}, m·s^{-1}	0.0164			0.0167
x_0, –	0.0036			

* refers to experiments with ammonia addition

Table 2. Input parameters – full-scale experiments

Parameter	WTP at Strumień		WTP at Dziećkowice		WTP at Goczałkowice	
	A	B	C	D	E	F
$[O_3]_{G,0}$, mol·m^{-3}	3.46×10^{-1}	3.46×10^{-1}	1.17×10^{-1}	1.16×10^{-1}	1.44×10^{-1}	1.48×10^{-1}
$[DOC]_0$, mol·m^{-3}	2.38×10^{-1}	1.28×10^{-1}	1.55×10^{-1}	1.68×10^{-1}	2.11×10^{-1}	2.23×10^{-1}
$[H^+]_0$, mol·m^{-3}	7.94×10^{-5}	3.98×10^{-5}	1.99×10^{-6}	1.26×10^{-6}	2.51×10^{-5}	5.01×10^{-5}
$[OH^-]_0$, mol·m^{-3}	1.26×10^{-4}	2.51×10^{-4}	5.01×10^{-3}	7.94×10^{-3}	3.98×10^{-4}	1.99×10^{-4}
$[Br^-]_0$, mol·m^{-3}	1.23×10^{-3}	9.06×10^{-4}	4.14×10^{-4}	8.54×10^{-4}	1.15×10^{-3}	1.27×10^{-3}
$[PO_4^{3-}]_0$, mol·m^{-3}	1.09×10^{-2}	0.76×10^{-2}	2.17×10^{-2}	1.85×10^{-2}	0.94×10^{-2}	0.73×10^{-2}
$[HCO_3^-]_0$, mol·m^{-3}	1.1	0.8	1.4	1.3	1.13	1.15
$[CO_3^{2-}]_0$, mol·m^{-3}	0	0	0.83	0.69	0.05	0
$[NH_4^+]_0$, mol·m^{-3}	7.78×10^{-3}	3.33×10^{-3}	2.22×10^{-3}	5.56×10^{-4}	4.61×10^{-2}	4.33×10^{-2}
$[NH_3]_0$, mol·m^{-3}	0	0	0	0	3.53×10^{-3}	5.88×10^{-4}
T, K	291.1	291.6	293.5	294.8	283.1	284.0
D_{O_3}, m^2·s^{-1}	1.63×10^{-9}	1.66×10^{-9}	1.74×10^{-9}	1.76×10^{-9}	1.29×10^{-9}	1.33×10^{-9}
d_b, m	0.003[a]	0.005	0004	0.004	0.006	0.006
	0.004					
k_La s^{-1}	counter-current flow mode					
	–	0.0016	0.0124	0.0028	0.0069	0.0066
	co-current flow mode					
	0.0024	0.0015	0.0096	0.0023	–	–
H_e, Pa·m^3·mol^{-1}	9.08×10^6	9.31×10^6	10.25×10^6	10.81×10^6	5.96×10^6	5.93×10^6
H, m	3.69	3.62	9.00	6.20	8.50	13.00
D_{LL}, m^2·s^{-1}	7.04×10^{-3}	4.31×10^{-3}	4.35×10^{-2}	1.08×10^{-2}	1.91×10^{-2}	5.12×10^{-2}
ε_G, –	0.058[a]	0.004[b]	0.028[b]	0.007[b]	0.023[b]	0.022[b]
	0.006[c]	0.004[c]	0.021[c]	0.006[c]	–	–
ε_L, –	0.942[a]	0.996[b]	0.972	0.993[b]	0.977	0.978
	0.994	0.996[c]	0.979[c]	0.994[c]	–	–
u_L, m·s^{-1}	1.48[a]	0.0119	0.0281	0.0185	0.0214	0.0292
	0.0189					
u_{G_0}, m·s^{-1}	0.1063[a]	0.0008	0.0053	0.0013	0.0045	0.0041
	0.0014					
x_0, –	0.0065	0.0065	0.0059	0.0062	0.0075	0.0075

a – refers to the vertical pipe; b – refers to the counter- current flow mode; c – refers to the co-current flow mode

Simulating the performance of the full-scale facilities was more intrinsic. A division into segments of the different flow mode was required. The ozone mass transfer from the gas phase to the liquid phase was considered only in segments where gas dissolution was performed. The results obtained at the outlet from the first segment were declared as initial boundary conditions for the second one and so on.

The dispersion coefficient was computed based on the overall vessel dispersion number considering an artificial velocity relevant to that segment, as there was no possibility to perform tracer tests in an open-open mode.

3.2. Model validation results

To validate the model, thirteen independent sets of experimental data were used as input. Simulations were carried out as described in Part I (Olsińska, 2019).

The results of the model validation with the data obtained in experiments conducted under laboratory conditions are shown in Fig. 2. It can be seen that bromate concentration was predicted well by the model with a resulting TIC value of 0.110–0.174 for the basic model and the model developed for the case of water ammonification, respectively. A TIC value lower than 0.3 confirmed a good agreement between computed and measured data (Audenaert et al., 2010). A slight overestimation of bromate formation was observed with a negative relative deviation of 12–50%. But, given that a satisfactory kinetic-based model should predict BrO_3^- concentration within a relative deviation $\Delta = \pm 100\%$ of the measured value (von Gunten, 2003), the results may be considered as acceptable.

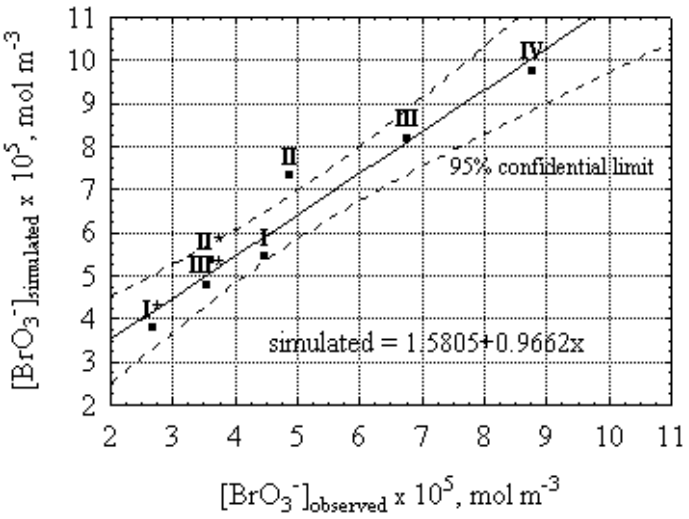

Fig. 2. Results of model validation with laboratory-scale experiments

The overprediction of the actual bromate concentrations may probably be partially attributed to the values of liquid phase volumetric mass transfer coefficients used at this stage of the research. The values of k_La (Tab. 1) are close to those reported by Akita and Yoshida (1974), Haut and Cartage (2005), but they are almost one order higher than the values obtained by Biń et al. (2001), Mizumo and Tsuno (2010) or Rhim and Yoon (2005), and those of the full-scale units tested in this study (Table 2). Thus, it seems that further research is required to assess an actual effect of the volumetric mass transfer coefficient on bromate formation.

Moreover, the results of the laboratory experiments agreed well with general knowledge on bromate formation (von Gunten, 2003; Olsińska, 2003). For example, comparing data sets in pairs – with and without ammonia addition – one may observe that the formation of bromate during ozonation was limited in the presence of ammonia.

A reasonably good conformity between the simulated and measured bromate concentrations was obtained in the full-scale tests as well (Tab. 3). For this relatively small sample pool, the observed and simulated values agreed well and bromate concentration was predicted with the mean absolute percentage error of

16–42%. It is at least two times lover than the relative residuals achieved by Hassan et al. (2003). This may be due to the introduction of NOM to the reaction system and addition of hydrodynamic phenomena to the kinetic model.

Table 3. Results of model validation with full-scale experiments

WTP	$[BrO_3^-]$, mol·m^{-3}			
	Measured	STD	Simulated	Deviation (RMSE = 1.98; TIC = 0.142)
A	2.81×10^{-5}	$\pm 7.819 \times 10^{-6}$	4.46×10^{-5}	-1.65×10^{-5}
B	2.97×10^{-5}	$\pm 7.819 \times 10^{-6}$	5.00×10^{-5}	-2.03×10^{-5}
C	3.83×10^{-5}	$\pm 7.819 \times 10^{-6}$	5.32×10^{-5}	-1.49×10^{-5}
D	1.00×10^{-4}	$\pm 9.382 \times 10^{-6}$	1.19×10^{-4}	-1.88×10^{-5}
E	1.64×10^{-5}	$\pm 7.037 \times 10^{-6}$	2.81×10^{-5}	-1.17×10^{-5}
F	1.09×10^{-5}	$\pm 7.037 \times 10^{-6}$	1.72×10^{-5}	-6.25×10^{-6}

On the one hand, the deviations between the predicted and measured values can be attributed to the inaccuracy in measurements of bromate ions as they were experienced at low concentrations (ppb levels). Similarly, an experimental determination of the dispersion number at the full-scale facilities also posed some difficulties. On the other hand, no consideration was given to differences in the nature of the organic matter in the water taken from different sources. However, some equations for NOM reacting with molecular ozone and hydroxyl radicals, hypobromite and hypobromous acid were added to the model, the coefficients in the rate expressions were assumed to have identical values for water taken from different sources. Moreover, ozone consumption due to microorganism inactivation and its reactions with inorganic species as (NO_2^-, Fe^{2+}, Mn^{2+}, SO_3^{2-}) or organic micropollutants were neglected in this study. These reactions may affect the amount of oxidizing species available in the reactions leading to bromate formation (von Sontag and von Gunten, 2012).

In general, the model was found to provide good agreement with the experimental data under most conditions tested despite the simplifying assumptions made (Olsińska, 2019). The above results show that the proposed model is robust and can handle different water characteristics and different experimental conditions.

4. CONCLUSIONS

The proposed model was positively verified as a promising tool for prediction of bromate formation in natural waters during the ozonation process performed with and without ammonia addition. The predictive abilities were proved by the model validation carried out with experimental results obtained both in laboratory tests and full-scale experiments. A good conformity between the simulated bromate concentrations and experimental observations was demonstrated upon the conventional ozonation process run under different hydrodynamic conditions.

Although the model fitted well the experimental data, further research is required to quantify the reactions between NOM and oxidizing species present in water during ozonation, to confirm its applicability for different NOM sources. A model with more specific reactions of ozone, hydroxyl radicals and bromine with hydrophilic and hydrophobic fractions of NOM will be developed.

SYMBOLS

a	specific gas–liquid interfacial area, $m^2 \cdot m^{-3}$
ADM	axial dispersion model
d	diameter, m
D_L	axial (longitudinal) dispersion coefficient, $m^2 \cdot s^{-1}$
DOC	dissolved organic carbon, $mol \cdot C \cdot m^{-3}$
DBP	disinfection by-product
H	water head measured from the level of ozone diffuser to water surface
H_e	Henry's law constant, $Pa \cdot mol^{-1} \cdot m^3$
$k_L a$	liquid phase volumetric mass transfer coefficient, s^{-1}
NOM	natural organic matter
$[O_3]_L$	concentration of dissolved ozone in the bulk liquid, $mol \cdot m^{-3}$
RMSE	root mean-square error
STD	standard deviation, $mol \cdot m^{-3}$
T	temperature, K
TFG	Tomiyasu, Fukutomi and Gordon
TIC	Theil's inequality coefficient, –
u	superficial velocity, $m \cdot s^{-1}$
u_p	terminal bubble rise velocity, $m \cdot s^{-1}$
u_S	slip velocity, $m \cdot s^{-1}$
WTP	Water Treatment Plant
x	gas molar fraction in the gas phase, –

Greek symbols

ε	hold-up coefficient, –
Δ	relative deviation, %

Subscripts

b	refers to gas bubbles
L	refers to the liquid phase
G	refers to the gas phase
0	refers to initial values

REFERENCES

Akita K., Yoshida F., 1974. Bubble size, interfacial area and liquid phase mass transfer coefficients in bubble columns. *Ind. Eng. Chem. Process Des. Dev.*, 13, 84?91. DOI: 10.1021/i260049a016.

Audenaert W.T.M., Callewaert M., Nopens I., Cromphout J., Vanhoucke R., Dumoulin A., Dejans P., Van Hulle S.W.H., 2010. Full-scale modelling of an ozone reactor for drinking water treatment. *Chem. Eng. J.*, 157, 551–557. DOI: 10.1016/j.cej.2009.12.051.

Biń A.K., Duczmal B., Machniewski P., 2001. Hydrodynamics and ozone mass transfer in a tall bubble column. *Chem. Eng. Sci.*, 56, 6233–6240. DOI: 10.1016/S0009-2509(01)00213-5.

Calderbank P.H., 1967. *Gas absorption from bubbles*. 3^{rd} edition, IChemE, London.

Chowdhury S., Champagne P., McLellan P.J., 2009. Models for predicting disinfection byproduct (DBP) formation in drinking waters: A chronological review. *Sci. Tot. Env.*, 407, 4189-4206. DOI: 10.1016/j.scitotenv.2009.04.006.

Clift R., Grace J. R., Weber M.E., 1978. *Bubbles, drops and particles*. Academic Press Inc., New York.

Davidson J. F., Harrison D., 1966. The behavior of a continuity bubbling f1uidized bed. *Chem. Eng. Sci*., 21, 731–738. DOI: 10.1016/0009-2509(66)870001-x.

Griffith P., Wallis G.B., 1961. Two-phase slug flow. *J. Heat Transfer*, 83, 307?318. DOI: 10.1115/1.3682268.

Harmathy T. Z., 1960. Velocity of large drops and bubbles in media of infinite or restricted extent. *AIChE J*., 6, 281–288. DOI: 10.1002/aic.690060222.

Hassan K. Z. A., Bower K. C., Miller C. M., 2003. Numerical simulation of bromate formation during ozonation of bromide. *J. Environ. Eng.*, 129 (11), 991–998. DOI: 10.1061/(ASCE)0733-9372(2003)129:11(991).

Haut B., Cartage T., 2005. Mathematical modeling of gas-liquid mass transfer rate in bubble columns operated in the heterogeneous regime. *Chem. Eng. Sci*., 60, 5937–5944. DOI: 10.1016/j.ces.2005.04.022.

Hinze J. O., 1955. Fundamentals of the hydrodynamic mechanism of sliding in dispersion processes. *AIChE J*., 1, 289?295. DOI: 10.10002/aic.690010303.

ISO 11206:2011. *Water quality – Determination of dissolved bromate – Method using ion chromatography (IC) and post column reaction (PRC)*. Technical Committee: ISO/TC 147/SC 2 Physical, chemical and biochemical methods.

Jarvis P., Parsons S.A., Smith R., 2007. Modeling bromate formation during ozonation. *Ozone Sci. Eng*., 29, 429?442. DOI: 10.1080/01919510701643732.

Lapidus L., Elgin J.C., 1957. Mechanics of vertical moving fluidised systems. *AIChE J*., 3, 63–68. DOI: 10.1002/aic.690030112.

Levenspiel O., 1999. *Chemical reaction engineering*. John Wiley & Sons, 3^{rd} edition, New York.

Mariñas B.J., Liang S., Aieta E.M., 1993. Modelling hydrodynamics and ozone residual distribution in a pilot-scale ozone bubble-diffuser contractor. *J. Am. Water Works Assn.*, 85, 90–99. DOI: 10.1002/j.1551-8833.1993.tb05960.x.

Mizumo T., Tsuno H., 2010. Evaluation of solubility and the gas-liquid equilibrium coefficient of high concentration gaseous ozone to water. *Ozone Sci. Eng*., 32, 3–15. DOI: 10.1080/01919510903482376.

Olsińska U., 2002. Influence of contactor hydrodynamic behaviour on the efficiency of the ozonation process. *Polish J. Chem. Technol*., 2(4), 21–27.

Olsińska U., 2003. Modelling of bromate formation in relation to hydrodynamic characteristics of ozone contactors, In: Pawłowski L., Dudzińska M.R., Pawłowski A. (Eds.) *Environmental Engineering Studies*. Springer, Boston, MA, 109–119. DOI: 10.1007/978-1-4419-8949-9_12.

Olsińska U., 2019. Numerical modelling of ozonation process with respect to bromate formation. Part I – Model development. *Chem. Process Eng.*, 40, 21–38. DOI: 10.24425/cpe.2018.124994.

Rhim J.A., Yoon J.H., 2005. Mass transfer characteristics and overall mass transfer coefficient in the ozone contactor. *Korean J. Chem. Eng*., 22, 201–207. DOI: 10.1007/BF02701485.

Roustan M., Beck C., Wable O., Duguet J. P., Mallevialle J., 1993. Modelling hydraulics of ozone contactors. *Ozone Sci. Eng*., 15, 213–226. DOI: 10.1080/01919519308552485.

Sadiq R., Rodriguez M.J., 2004. Disinfection by-products (DBPs) in drinking water and predictive models for their occurrence: a review. *Sci. Total Environ.*, 321, 21–46. DOI: 10.1016/j.scitotenv.2003.05.001.

Turner J. C. R., 1966. On bubble flow in liquids and fluidized beds. *Chem. Eng. Sci*., 21, 971?974. DOI: 10.1016/0009-2509(66)85094-7.

von Gunten U., 2003. Ozonation of drinking water: Part II. Disinfection and by-product formation in presence of bromide, iodide or chlorine. *Water Res*., 37, 1469–1487. DOI: 10.1016/S0043-1354(02)00458-x.

von Sonntag C., von Gunten U., 2012. *Chemistry of ozone in water and wastewater treatment – from basic principles to applications*. IWA Publishing, London.

Received 18 November 2018
Received in revised form 14 January 2019
Accepted 15 January 2019